acta physica slovaca vol. 48 No. 1, 13 – 22 February 1998

RELATIVISTIC MEAN FIELD APPROACH TO SUPERHEAVY NUCLEI

Štefan Gmuca
Institute of Physics, Slovak Academy of Sciences, Dúbravská cesta 9, SK-842 28 Bratislava, Slovakia

Received 3 September 1997, in final form 27 December 1997, accepted 12 January 1998

The relativistic mean field theory with the scalar selfinteraction has been applied to the self-consistent calculation of ground state properties of superheavy nuclei. The binding energies, single particle proton and neutron levels, densities and other observables are analyzed for nuclei with large proton and neutron numbers. The positions of the magic gaps in the superheavy region are evaluated and compared with other self consistent calculations. The implications on the stability of superheavy nuclei are discussed.

1. Introduction

The discoveries of several new superheavy elements with atomic numbers as large as $Z = 112$ have been reported recently [1, 2, 3, 4, 5, 6]. These elements are already very close to the alleged island of stability in the superheavy region (Z=114). Although the synthesis and detection of new superheavy nuclei is confronted with enormous difficulties, experimental efforts are being made currently at the laboratories in GSI, Dubna, Berkeley and GANIL [7].

Among various theoretical approaches to the heaviest elements, the macroscopic–microscopic methods [8, 9, 10] are most often used to calculate and predict the properties of superheavy nuclei. Usually, one of the variants of the liquid drop model is used as the macroscopic part of this approach. The microscopic part usually involves models based on a single–particle picture. The detailed review of the macroscopic–microscopic approaches can be found elsewhere (see e.g. [9] and references therein). However, the macroscopic–microscopic approach, despite its success, is only an approximation to the self–consistent theories (e.g. Hartree–Fock) and suffers from the lack of their self–consistent coupling between the macroscopic and microscopic contributions to the total energy. In particular, the macroscopic–microscopic method requires some *a priori* knowledge about the densities and single–particle potentials expected. This may break down when extrapolating into the unknown region of superheavy nuclei where more complicated density dependences may occur. Such effects are naturally included in the self–consistent nuclear models.

The models based on self-consistent theories (e.g. Skyrme–Hartree–Fock or relativistic mean-field approaches) are certainly much more suitable for the calculations of structure of nuclei. Until very recently, however, the self-consistent models were applied only scarcely for large-scale calculations of superheavy nuclei; their applications were limited mostly to calculations of some specific features of superheavy nuclei. In addition, the predictive power of the effective interactions used was not sufficient for reliable conclusions.

Recently the ground-state properties of the superheavy elements with $108 \le Z \le 128$ and $150 \le N \le 192$ were investigated using the Skyrme–Hartree–Fock method [11] and the relativistic Hartree–Bogoliubov calculations were performed for nuclei with $Z = 110-114$ and $N = 154-190$ [12]. Both studies have demonstrated the ability of the current self-consistent approaches to be competitive with the macroscopic–microscopic methods for the calculations of superheavy elements.

The nonlinear relativistic mean-field theory (RMFT) [13] has already been proven to be a reliable tool for the calculations of ground-state properties of finite nuclei in the vicinity of the valley of stability (see e.g. [15] and references therein). The aim of the present work is to apply the RMFT theory to the prediction of properties of exotic superheavy elements and to study the problem of their shell stability. The paper is organized as follows. The relativistic mean field theory is briefly described in Sec. 2. Sec. 3 is devoted to the results obtained and their discussion. In subsection 3.1 the single-particle structure of the superheavy nuclei is investigated. Subsection 3.2 contains the results concerning the density distributions of superheavy elements. Q_α values and implications for the stability of superheavy nuclei are discussed in subsection 3.3. Finally, conclusions are contained in Sec. 4.

2. RMFT

Our starting point is the Lagrangian density which includes the baryon field (ψ), neutral scalar and vector meson fields (σ, ω), the isovector $\boldsymbol{\rho}$ meson field together with an electromagnetic interaction in a renormalizable field theory. In addition, the cubic and quartic self-interactions of the scalar meson field have been added to allow the model enough flexibility in describing nuclear properties.

The full Ladrangian density reads

$$\begin{aligned}\mathcal{L} &= \overline{\psi}(i\gamma_\mu\partial^\mu - M)\psi \\ &+\frac{1}{2}\partial_\mu\sigma\partial^\mu\sigma - \frac{1}{2}m_\sigma^2\sigma^2 - U(\sigma) + g_\sigma\overline{\psi}\psi\sigma \\ &-\frac{1}{4}\omega_{\mu\nu}\omega^{\mu\nu} + \frac{1}{2}m_\omega^2\omega_\mu\omega^\mu - g_\omega\overline{\psi}\gamma_\mu\psi\omega^\mu \\ &-\frac{1}{4}\boldsymbol{\rho}_{\mu\nu}\boldsymbol{\rho}^{\mu\nu} + \frac{1}{2}m_\rho^2\boldsymbol{\rho}_\mu\boldsymbol{\rho}^\mu - g_\rho\overline{\psi}\gamma_\mu\boldsymbol{\tau}\psi\boldsymbol{\rho}^\mu \\ &-\frac{1}{4}F_{\mu\nu}F^{\mu\nu} - e\overline{\psi}\gamma_\mu\frac{(1-\tau_3)}{2}\psi A^\mu, \end{aligned} \tag{1}$$

where the symbols used have their usual meaning [14].

The first line of eq.(1) describes the nucleon (ψ) part of the Lagrangian density. The second line is the standard scalar σ-meson term with cubic and quartic selfinteractions

$$U(\sigma) = \frac{1}{3}b_\sigma M(g_\sigma\sigma)^3 + \frac{1}{4}c_\sigma(g_\sigma\sigma)^4. \tag{2}$$

The strengths of these selfcouplings are given by the dimensionless constants b_σ and c_σ. The third line contains the vector ω-meson part of $\mathcal{L}$. The fourth line represents the contribution of the isovector $\boldsymbol{\rho}$ field and the last line describes the electromagnetic interaction. The field tensors are given by usual expessions

$$\begin{aligned}\omega^{\mu\nu} &= \partial^\mu\omega^\nu - \partial^\nu\omega^\mu \\ \boldsymbol{\rho}^{\mu\nu} &= \partial^\mu\boldsymbol{\rho}^\nu - \partial^\nu\boldsymbol{\rho}^\mu \\ F^{\mu\nu} &= \partial^\mu A^\nu - \partial^\nu A^\mu. \end{aligned} \tag{3}$$

In the following we restrict ourselves to the mean field (i.e. meson fields are replaced by their expectation values) and no-sea (i.e. we neglect the effects of antiparticles) approximations. In addition, we suppose the spherical symmetry which greatly simplifies numerical evaluations. As a consequence, only the time-like components ($\omega_0(r)$ and $\rho_{00}(r)$) of the vector meson fields ω_μ and $\rho_{\mu\nu}$ survive. The space-like components vanish identically.

Using the usual ansatz for the Dirac single-particle spinors [14]

$$\psi_\alpha(\boldsymbol{r}) = \psi_{ljm}(\boldsymbol{r}) = \frac{1}{r}\begin{bmatrix} iG_{lj}(r)\Phi_{ljm}(\hat{\boldsymbol{r}}) \\ -F_{lj}(r)\Phi_{\bar{l}jm}(\hat{\boldsymbol{r}}) \end{bmatrix} \tag{4}$$

with $\bar{l} = j \pm 1/2$ for $l = j \mp 1/2$ and $\Phi_{ljm}(\hat{\mathbf{r}})$ being the spinor spherical harmonics [14] we obtain the following coupled pair of radial Dirac equations for the upper (G_α) and lower (F_α) components

$$\left(\frac{d}{dr} + \frac{\kappa}{r}\right)G_\alpha(r) = [M - U(r) - V(r) + \epsilon_\alpha]F_\alpha(r), \tag{5}$$

$$\left(\frac{d}{dr} - \frac{\kappa}{r}\right)F_\alpha(r) = [M - U(r) + V(r) - \epsilon_\alpha]G_\alpha(r). \tag{6}$$

The scalar potential $U(r)$ is given simply by

$$U(r) = g_\sigma\sigma(r), \tag{7}$$

while the vector potential $V(r)$ has a more complicated structure,

$$V(r) = g_\omega\omega_0(r) + g_\rho\tau_3\rho_{00}(r) + \frac{(1-\tau_3)}{2}eA_0(r). \tag{8}$$

Here α denotes the spin and angular quantum numbers and κ is the Dirac quantum number given by

$$\kappa = \begin{cases} -(j+1/2) & \text{for} \quad j = l + 1/2 \\ +(j+1/2) & \text{for} \quad j = l - 1/2. \end{cases} \tag{9}$$

The quantity $\tau_3 = +1$ for neutrons and $\tau_3 = -1$ for protons.

The meson and photon fields obey the radial Laplace equations

$$\left(\frac{d^2}{dr^2} - m_\sigma^2\right)[r\sigma(r)] = -g_\sigma r\left\{\rho_S(r) - b_\sigma M\left[g_\sigma\sigma(r)\right]^2 - c_\sigma\left[g_\sigma\sigma(r)\right]^3\right\}, \quad (10)$$

$$\left(\frac{d^2}{dr^2} - m_\omega^2\right)[r\omega_0(r)] = -g_\omega r\rho_B(r), \quad (11)$$

$$\left(\frac{d^2}{dr^2} - m_\rho^2\right)[r\rho_{00}(r)] = -g_\rho r\rho_B^{(3)}(r), \quad (12)$$

$$\frac{d^2}{dr^2}[rA_0(r)] = -er\rho_B^{(p)}(r), \quad (13)$$

where the sources are determined by the corresponding densities in the static nucleus. Namely,

$$\rho_S(r) = \sum_\alpha^{occ.}\bar{\psi}_\alpha(\mathbf{r})\psi_\alpha(\mathbf{r}) = \sum_\alpha^{occ.}\frac{(2j_\alpha+1)}{4\pi r^2}\left[G_\alpha^2(r) - F_\alpha^2(r)\right], \quad (14)$$

$$\rho_B(r) = \sum_\alpha^{occ.}\psi_\alpha^\dagger(\mathbf{r})\psi_\alpha(\mathbf{r}) = \sum_\alpha^{occ.}\frac{(2j_\alpha+1)}{4\pi r^2}\left[G_\alpha^2(r) + F_\alpha^2(r)\right], \quad (15)$$

$$\rho_B^{(3)}(r) = \sum_\alpha^{occ.}\psi_\alpha^\dagger(\mathbf{r})\tau_3\psi_\alpha(\mathbf{r}) = \sum_\alpha^{occ.}\frac{(2j_\alpha+1)}{4\pi r^2}\tau_{3\alpha}\left[G_\alpha^2(r) + F_\alpha^2(r)\right], \quad (16)$$

$$\rho_B^{(p)}(r) = \sum_\alpha^{occ.}\psi_\alpha^\dagger(\mathbf{r})\frac{(1-\tau_3)}{2}\psi_\alpha(\mathbf{r}) = \sum_\alpha^{occ.}\frac{(2j_\alpha+1)}{4\pi r^2}\frac{(1-\tau_{3\alpha})}{2}\left[G_\alpha^2(r) + F_\alpha^2(r)\right], \quad (17)$$

where we adopt the following single–particle wave function normalization

$$\int_0^\infty\left[G_\alpha^2(r) + F_\alpha^2(r)\right]dr = 1. \quad (18)$$

An expression for the total energy of the finite system can be derived from the Lagrangian (1) in the standard way [14, 15]. After some manipulations we finally obtain the following formula

$$E_{\mathrm{RMFA}} = \sum_\alpha(2j_\alpha+1)\epsilon_\alpha + \frac{1}{2}\int d\mathbf{r}\left\{g_\sigma\sigma(r)\rho_S(r) - \frac{1}{3}b_\sigma M[g_\sigma\sigma(r)]^3 \right. \quad (19)$$
$$\left. - \frac{1}{2}c_\sigma[g_\sigma\sigma(r)]^4 - g_\omega\omega_0(r)\rho_B(r) - eA_0(r)\rho_B^{(p)}(r)\right\}.$$

In addition, this energy should be corrected for the spurious centre–of–mass (c.m.) motion. The nonrelativistic harmonic oscillator estimate for the c.m. energy correction $E_{c.m.} = -\frac{3}{4}41A^{-1/3}$ was used. In the case of the calculations of the open shell nuclei,

Table 1. Coupling constants and masses for the non-linear parameter set NL-SH [16] and derived nuclear matter properties.

Masses	Coupling constants
m_σ = 526.059 MeV	g_σ = 10.444
	b_σ = 0.0012746
	c_σ = −0.0013308
m_ω = 783.000 MeV	g_ω = 12.945
m_ρ = 763.000 MeV	g_ρ = 4.383
M = 939.000 MeV	
Nuclear matter properties	
ρ_0	0.146 fm^{-3}
$(E/A)_\infty$	16.43 MeV
K	355 MeV
J	36.1 MeV
M^*/M	0.60

the schematic BCS pairing was applied using a constant pairing gap formalism and the pairing energy has been added to the total energy.

The set of equations presented in this section have to be solved by iteration up to the self–consistency is achieved.

The RMFT calculations have been performed using the NL–SH [16] parameter set. Tha values of the parameters and the nuclear matter properties obtained in the calculations using them are listed in Table 1. This set gives a very good description of nuclei along the stability line as well as of neutron–rich nuclei. This can be largely attributed to the proper isovector properties of the parameter set used with an asymmetry energy $J \sim 36$ MeV.

3. Results and discussion

3.1. Single–particle levels

The single–particle level structure close to the Fermi surface strongly influences the stability properties of nuclei at the ground–state. The position of the magic gaps in the superheavy nuclei region is of great interest as it is believed that around the doubly magic nuclei the island of stability should exist. These expectations are based primarily upon phenomenological models such as the Woods–Saxon single–particle potential with the universal variant of parameters [17] or the folded–Yukawa single–particle potential [8, 9, 10]. The Z=114 and N=184 are expected to be the magic numbers in the region of the superheavy elements.

The superheavy nuclei are expected to be axially and reflection symmetric or spherical in their ground state [19]. The macroscopic–microscopic calculations have indicated that the isotones along the N=184 line are spherical [9] and the isotopes with Z=114

Single-Particle Levels of Nuclei with Z=114

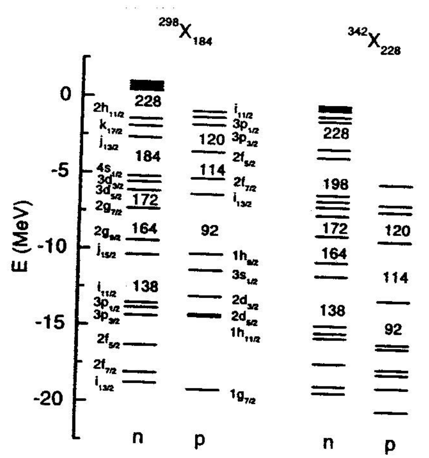

Fig. 1. Spherical neutron and proton single particle levels in $^{298}114_{184}$ and $^{342}114_{228}$ nuclei predicted in the RMFT approach.

are spherical [19] or only weakly deformed [9]. We have thus restricted our calculations to spherical nuclei only, which are much easier maintained.

We have performed a rather extensive study of the spherical single–particle spectra for the superheavy nuclei using the RMFT approach with the NL–SH parameters. The results obtained are illustrated in Fig. 1 for the $^{298}114$ and $^{342}114$ nuclei. This figure exhibits general features of the proton and neutron single–particle levels obtained in our calculations.

For the neutrons, the big shell gap at N=184 can be seen. The next large spherical shell closure is predicted at N=228. These results agree well with other self–consistent calculations (both, relativistic and nonrelativistic) [11, 12, 18] and phenomenological approaches [8],which also predict the neutron magic numbers at superheavy nuclei region to be N=184 and N=228. However, below N=184, two smaller gaps for N=164 and N=172 can be seen in our calculations.

For the protons, we found the large shell gap at Z=138. The proton numbers Z=114 and Z=120 also exhibit large gaps around 1.8 MeV. Smaller, however, still well profound shell gap can be seen at Z=106. The results obtained agree with the phenomenological calculations [19, 8], where the magic gap at Z=114 was observed, and are consistent with other RMFT calculations in which the shell closure at Z=114 [12, 18] and Z=120 [18] were also predicted. However, we have not obtained any indication of the shell closure at Z=126 as in ref. [11], where the extensive Skyrme–Hartree–Fock calculations of superheavy nuclei with various Skyrme forces were performed.

The present RMFT calculations suggest that the $^{298}114_{184}$ and $^{304}120_{184}$ nuclei are of doubly magic character; the next doubly magic superheavy nucleus should be

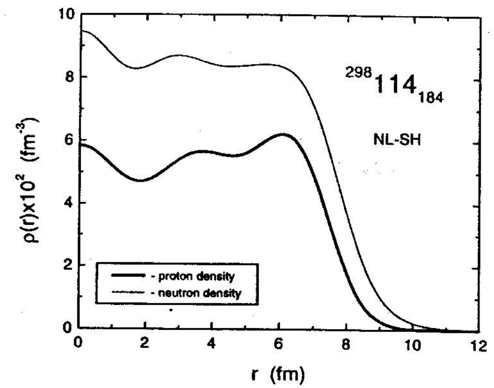

Fig. 2. Proton (thick line) and neutron (thin line) densities for the $^{298}114$ nucleus as predicted by RMFT with the NL–SH parameters.

$^{356}138_{228}$. Taking into account an observed region of enhanced stability for nuclei near deformed shells Z=106–108 and N=162–164 [7] (see shell gaps for Z=106 and N=164 in our spherical RMFT calculations), the pronounce shell gap at N=172 opens the possibility that the $^{286}114_{172}$ nucleus may also possesses an enhanced stability. This is an important fact for searching the superheavy elements, as the $^{286}114_{172}$ may be reached by a suitable combination of target and projectile nuclei (see [7]), while there is no such a combination to reach the doubly magic $^{298}114_{184}$ one at present.

3.2. Neutron and proton densities

Nucleon densities of superheavy elements resemble those of neutron–rich nuclei. In Fig. 2 we consider the nucleus $^{298}114$ with Z=114 and N=184. Here we have for the ratio of the densities $\rho_n/\rho_p \sim 1.5$ over the interior of the nucleus and larger for $r > 7$ fm. The additional neutrons form the neutron skin around the core of the nucleus; its thickness is ~0.28 fm if measured as a difference of neutron and proton root–mean–square (rms) radii.

In Fig. 3 we see the effect of removing 2 valence neutrons $(2\nu(4s_{1/2}))$ from the $^{298}114$ nucleus. The neutron density of the $^{296}114$ nucleus exhibits a strong depression in the centre of the nucleus, as the $s_{1/2}$ neutrons contribute mainly to the central region of the nucleus. This depression reaches almost 30%. One can also see that removing these 2 neutrons causes 15% depression in the proton density of the $^{296}114$ nucleus in comparison with the $^{298}114$ one.

3.3. Implications for the stability of superheavy elements

One of the most predominant mode of decay of the superheavy elements is α decay. The single most important quantity determining the α–decay half–lives is the Q_α value

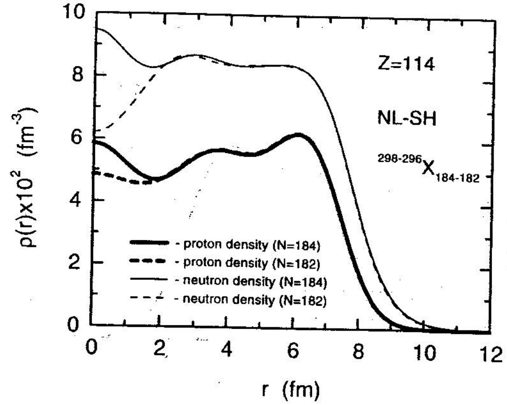

Fig. 3. Proton and neutron densities of ^{298}114 nucleus (solid lines) in comparison with densities of the ^{296}114 nucleus (dashed lines). One can see a deep central depression due to removing of two valence neutrons.

of the decay. The energy released by a nucleus with N neutrons and Z protons when it emits an α particle is given by

$$Q_\alpha(N,Z) = BE(2,2) - BE(N,Z) + BE(N-2,Z-2), \qquad (20)$$

where BE(N,Z) and BE(N-2,Z-2) stand for the binding energies of the parent and daughter nuclei, respectively and BE(2,2) is the experimental binding energy of the α–particle (BE(2,2)=28.296 MeV).

For the region of the enhanced stability the α–decay half–lives would be longer than for neighbour nuclei. The T_α depends on the Q_α very sensitively; the change of Q_α of 1 MeV may result in the change of T_α of several orders of magnitude. The α–decay half–lives may be evaluated by the phenomenological formula of Viola and Seaborg [20]

$$\log T_\alpha = (aZ+b)Q_\alpha^{-1/2} + (cZ+d), \qquad (21)$$

where Z is the atomic number of the parent nucleus and a, b, c, d are adjusted parameters given in [21]. T_α is expressed in seconds and Q_α in MeV.

We have calculated the Q_α values for many nuclei of the region of superheavy elements. The most interesting result is shown in Fig. 4. This indicates that the RMFT prediction for the Q_α value of the $^{286}114_{172}$ nucleus is much smaller than that of microscopic–macroscopic predictions. Smaller Q_α larger T_α; thus the $^{286}114_{172}$ nucleus may be a candidate for a new relatively long–living superheavy nucleus.

4. Summary and conclusions

We have investigated the ground–state properties of superheavy nuclei using the relativistic mean–field approach with the NL–SH parameters. Predictions have been

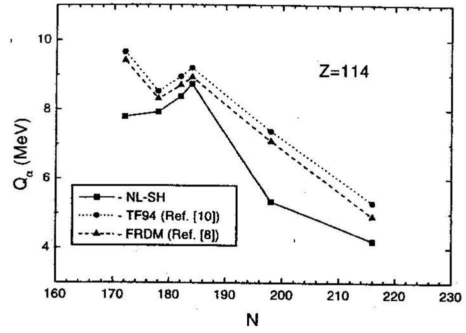

Fig. 4. Q_α values for Z=114 isotopic chain as calculated by RMFT in comparison with microscopic–macroscopic calculations.

made for single–particle spectra, neutron and proton densities. The Q_α values have been calculated for some closed shell nuclei. The results indicate that nuclei with Z=114 and Z=120 exhibit an enhanced stability. The analysis of Q_α values suggests that the $^{286}114_{172}$ nucleus may have longer life–time in comparison with the microscopic–macroscopic predictions.

Acknowledgements This work was supported in part by the VEGA agency under grant nos. 95/5305/645 and 2/1155/97.

References

[1] S. Hofmann, V. Ninov, F.P. Hessberger, P. Armbruster, H. Folger, G. Münzenberg, H.J. Schött, A,G. Popeko, A.V. Yeremin, A.N. Andreyev, S. Saro, R. Janik, M. Leino: *Z. Phys.* **A350** (1995) 277; ibid., p. 281

[2] S. Hofmann, V. Ninov, F.P. Hessberger, P. Armbruster, H. Folger, G. Münzenberg, H.J. Schött, A,G. Popeko, A.V. Yeremin, S. Saro, R. Janik, M. Leino: *Z. Phys.* **A354** (1996) 229

[3] A. Ghiorso, D. Lee, L.P. Somerville, W. Loveland, J.M. Nitschke, W. Ghiorso, G.T. Seaborg, P. Wilmarth, R. Leres, A. Wydler, M. Nurmia, K. Gregorich, K. Czerwinski, R. Gaylord, T. Hamilton, N.J. Hannink, D.C. Hoffman, C. Jarzynski, C. Kacher, B. Kadkhodayan, S. Kreek, M. Lane, A. Lyon, M.A. McMahan, M. Neu, T. Sikkeland, W.J. Swiatecki, A. Türler, J.T. Walton, S. Yashita: *Nucl. Phys.* **A583** (1995) 861c; *Phys. Rev.* **C51** (1995) R2293

[4] Y.T. Oganessian: *Nucl. Phys.* **A583** (1995) 823c

[5] Yu.A. Lazarev, Yu.V. Lobanov, Yu.S. Oganessian, V.K. Utyonkov, F.Sh. Abdulin, G.V. Buklanov, B.N. Gikal, S. Iliev, A.N. Mezentsev, V.N. Polyakov, I.M. Sedykh, I.V. Shirokovsky, V.G. Subbotin, A.M. Sukhov, Yu.S. Tsyganov, V.E. Zhuchko, R.W. Lougheed, K.J. Moody, J.F. Wild, E.K. Hulet, J.H. McQuaid: *Phys. Rev. Lett.* **73** (1994) 624

[6] Yu.A. Lazarev *et al.*: *Phys. Rev. Lett.* **75** (1995) 1903

[7] Yu.Ts. Oganessian: *in Proc. 3rd Int. Conf. on Dynamical Aspects of Nuclear Fission, Častá Papiernička, Slovakia, Aug.30 Sept. 4, 1996*, eds. J. Kliman, B.I. Pustylnik (JINR Dubna, 1997) p. 8

[8] P. Möller, J.R. Nix: *Nucl. Phys.* **A549** (1992) 84

[9] P. Möller, J.R. Nix: *J. Phys. G* **20** (1994) 1681

[10] P. Möller, J.R. Nix, W.D. Myers, W.J. Swiatecki: *Atom. Data and Nucl. Data Tables* **59** (1995) 185

[11] S. Ćwiok, J. Dobaczewski, P.-H. Heenen, P. Magierski, W. Nazarewicz: *Nucl. Phys.* **A611** (1996) 211

[12] G.A. Lalazissis, M.M. Sharma, P. Ring, Y.K. Gambhir: *Nucl. Phys.* **A608** (1996) 202

[13] J. Boguta, A.R. Bodmer: *Nucl. Phys.* **A292** (1977) 413

[14] B.D. Serot, J.D. Walecka: *Adv. Nucl. Phys.* **16** (1986) 1

[15] Y.K. Gambhir, P. Ring, A. Thimet: *Ann. Phys.* **198** (1990) 132

[16] M.M. Sharma, M.A Nagarajan, P. Ring: *Phys. Lett. B* **317** (1993) 377

[17] S. Ćwiok, J. Dudek, W. Nazarewicz, J. Skalski, T. Werner: *Comput. Phys. Commun.* **46** (1987) 379

[18] K. Rutz, M. Bender, T. Bürvenich, T. Schilling, P.-G. Reinhard, J.A. Maruhn, W. Greiner: *Phys. Rev. C* **56** (1997) 238

[19] R. Smolańczuk: *Phys. Rev. C* **56** (1997) 812

[20] V.E. Viola, G.T. Seaborg: *J. Inorg. Nucl. Chem.* **28** (1966) 741

[21] A. Sobiczewski, Z. Patyk, S. Cwiok: *Phys. Lett.* **224B** (1989) 1